LA-UR-

Approved for public release;
distribution is unlimited.

Title: MCNP5 BENCHMARK CALCULATIONS FOR 3-D RADIATION TRANSPORT IN SIMPLE GEOMETRIES WITH VOID REGIONS

Author(s): Bryan Toth and Forrest B. Brown

Submitted to:

Form 836 (8/00)

Abstract

This report presents results for benchmark calculations performed using MCNP5. The benchmark problems consisted of simple geometries that contained at least one void region and one mono-energetic, isotropic, cubic source. Each configuration was simulated with a pure absorbing and a fifty-percent scattering medium. Fluxes were calculated at various points throughout the geometries. The calculations are compared to those performed by Kobayashi, Sugimura, and Nagaya, which can be found in 3-D Radiation Transport Benchmark Problems and Results for Simple Geometries with Void Regions [1]. The results for all three benchmarks performed matched those of Kobayashi within two standard deviations, a majority of which matched within one standard deviation.

Introduction

Accuracy is essential for simulations dealing with special nuclear materials; therefore, all new versions of MCNP must be verified by performing many different benchmark calculations that cover as many separate applications as possible. Flux distributions for 2-D void problems proved to be very difficult to determine as investigated by Ackroyd and Riyait [2]. This report focuses on MCNP5 benchmark calculations for flux at various points throughout simple geometries with void regions proposed by Kobayashi [3].

Three geometries are explored in this paper. All geometries have a mono-energetic, isotropic, cubic source, a void region, and a shield. The first geometry consists of three nested cubes with the source at the center bounded by a void region that is surrounded by a shield. The second geometry contains the source at the center with a straight void duct extending along one axis and surrounded by a shield. The third geometry is a source inside of a shielding rectangular prism with eight void ducts that each has three right-angled bends and leads outside of the shield. Vacuum boundary conditions exist for all configurations. Diagrams of the problems posed by Kobayashi are in figures 17-24 in the appendix.

The specific activity of the source is 1 n/cm^3-s. The total macroscopic cross section of the shield and source is 0.1 cm^{-1}, and the total macroscopic cross section of the void is 10^{-4} cm^{-1}. The macroscopic cross section of the void is non-zero to allow for comparison with 3-D transport codes that use the second order differential form. Each of the three geometries was simulated with pure absorbing media and then with 50% scattering media. Kobayashi [1] solved for the fluxes using numerical integration in the pure absorber cases and GMVP [4], a Monte-Carlo code, for the scattering cases.

Input Files

The input files are presented in the appendix. Input files that end in ‘a’ include detector sets A and B, and files that end in ‘b’ include detector set C. This division was necessary because MCNP5 limits the number of point detectors in one problem to 20. Input file that have a single ‘i’ are for the pure absorber case, and those files with ‘ii’ are for the 50% scattering case.

The problems posed by Kobayashi called for reflective boundaries on the x = 0, y = 0, and z = 0 planes; however, to use point detector estimators in MCNP5, reflective boundaries

cannot be present. To remedy this, the geometry was reflected in all three coordinate planes, giving the geometry symmetry about the origin and effectively multiplying most aspects of the problem by eight. The weight of each source particle was set to 8000 because of this multiplication in the geometry of the source. The source particle starting location was randomly determined within the 8000 cm^3 source with an equal probability of selection throughout the volume.

Because these problems called for imaginary materials with only macroscopic cross sections specified, two cross section libraries had to be created. The libraries specified microscopic cross sections for the arbitrary materials referred to as 99001 and 99002. Material 99001 was the pure absorber with a total microscopic cross section of 1 barn, which was detailed in the library file 'xs1' shown in the appendix. Material 99002 was the scattering shield with a total microscopic cross section of 1 barn and a scattering cross section of 0.5 barns, which was described in the library file 'xs2' also shown in the appendix. The macroscopic cross sections were adjusted by changing the atom density to meet the Kobayashi specifications. The file 'dir' was used to link to these libraries and appeared in the appendix.

Point detector estimators were used to obtain the desired fluxes. In the pure absorbing cases, the exclusion radii were set very low because there was not a possibility of a scattering event occurring near a detector; however, in the source, the exclusion radius was set to 1 cm because source particles that were generated in the vicinity of the detector would lead to wild variances and bad statistics in the tally from that detector. In the scattering cases, the exclusion radii were set to 5 cm, which was half of the mean free path of a neutron in the source or shield. Normally, this radius would be set to the mean free path of the particle, but to avoid the exclusion spheres crossing material boundaries, the exclusion radii had to be limited to only 5 cm. The large exclusion radius was necessary for the results to pass statistical checks.

To obtain accurate results and good statistics, only one million histories were needed for the cases without scattering, and no variance reduction was necessary. However, in the cases with scattering, anywhere from 10 to 200 million histories were needed in conjunction with some variance reduction for most of the results to pass statistical checks. In all of the scattering problems, implicit capture and cell importances were used to reduce the variance in the tallies. The splitting of the shield cell was also used along with importances to maintain data carriers from the source to the detectors in the extremities of the geometries.

Results

The calculations for the pure absorber cases were performed using the RSICC version 1.14 of MCNP5 on a Windows® PC. Calculations with scattering were performed using the LANL 1.13 version of MCNP5 on the Linux supercomputer lambda. Table 1 displays the calculated fluxes in the pure absorber case and compared those values to the analytical results that Kobayashi calculated, where FSD represents fractional standard deviation. Table 2 presents the fluxes for the 50 % scattering media and compared to the values calculated with GMVP. A negative percent difference in the tables represents when the MCNP5 result was less than the comparison value. Figures 1-16 display the fluxes relative to the analytical or GMVP results, respectively.

Table 1. Total flux for pure absorber cases

Case	Case i (no scattering)				
	Co-ordinates	Analytic method	MCNP5		
	(x,y,z) (cm)	Total Flux ($cm^{-2}s^{-1}$)	Total Flux ($cm^{-2}s^{-1}$)	FSD 1σ(%)	Difference (%)
1A	5,5,5	5.95659E+00	5.98076E+00	0.77	0.406
	5,15,5	1.37185E+00	1.37068E+00	0.16	-0.085
	5,25,5	5.00871E-01	5.00540E-01	0.10	-0.066
	5,35,5	2.52429E-01	2.52272E-01	0.09	-0.062
	5,45,5	1.50260E-01	1.50171E-01	0.08	-0.059
	5,55,5	5.95286E-02	5.94940E-02	0.08	-0.058
	5,65,5	1.53283E-02	1.53195E-02	0.07	-0.057
	5,75,5	4.17689E-03	4.17453E-03	0.07	-0.057
	5,86,5	1.18533E-03	1.18467E-03	0.07	-0.056
	5,95,5	3.46846E-04	3.46655E-04	0.07	-0.055
1B	5,5,5	5.95659E+00	5.98076E+00	0.77	0.406
	15,15,15	4.70754E-01	4.69752E-01	0.12	-0.213
	25,25,25	1.69968E-01	1.69789E-01	0.08	-0.105
	35,35,35	8.68334E-02	8.67671E-02	0.07	-0.076
	45,45,45	5.25132E-02	5.24800E-02	0.06	-0.063
	55,55,55	1.33378E-02	1.33296E-02	0.06	-0.061
	65,65,65	1.45867E-03	1.45775E-03	0.06	-0.063
	75,75,75	1.75364E-04	1.75251E-04	0.06	-0.064
	85,85,85	2.24607E-05	2.24459E-05	0.06	-0.066
	95,95,95	3.01032E-06	3.00831E-06	0.06	-0.067
1C	5,55,5	5.95286E-02	5.94940E-02	0.08	-0.058
	15,55,5	5.50247E-02	5.49859E-02	0.07	-0.071
	25,55,5	4.80754E-02	4.80398E-02	0.07	-0.074
	35,55,5	3.96765E-02	3.96514E-02	0.07	-0.063
	45,55,5	3.16366E-02	3.16198E-02	0.07	-0.053
	55,55,5	2.35303E-02	2.35187E-02	0.07	-0.049
	65,55,5	5.83721E-03	5.83408E-03	0.07	-0.054
	75,55,5	1.56731E-03	1.56645E-03	0.07	-0.055
	85,55,5	4.53113E-04	4.52860E-04	0.07	-0.056
	95,55,5	1.37079E-04	1.37003E-04	0.07	-0.055

	5,5,5	5.95659E+00	5.98076E+00	0.77	0.406
	5,15,5	1.37185E+00	1.37068E+00	0.16	-0.085
	5,25,5	5.00871E-01	5.00540E-01	0.10	-0.066
	5,35,5	2.52429E-01	2.52272E-01	0.09	-0.062
2A	5,45,5	1.50260E-01	1.50171E-01	0.08	-0.059
	5,55,5	9.91726E-02	9.91150E-02	0.08	-0.058
	5,65,5	7.01791E-02	7.01392E-02	0.07	-0.057
	5,75,5	5.22062E-02	5.21769E-02	0.07	-0.056
	5,86,5	4.03188E-02	4.02964E-02	0.07	-0.056
	5,95,5	3.20574E-02	3.20398E-02	0.07	-0.055
	5,95,5	3.20574E-02	3.20398E-02	0.07	-0.055
	15,95,5	1.70541E-03	1.70321E-03	0.13	-0.129
	25,95,5	1.40557E-04	1.40347E-04	0.15	-0.149
2B	35,95,5	3.27058E-05	3.26610E-05	0.14	-0.137
	45,95,5	1.08505E-05	1.08373E-05	0.13	-0.122
	55,95,5	4.14132E-06	4.13683E-06	0.12	-0.108
	5,5,5	5.95659E+00	5.98076E+00	0.77	0.406
	5,15,5	1.37185E+00	1.37068E+00	0.16	-0.085
	5,25,5	5.00871E-01	5.00540E-01	0.10	-0.066
	5,35,5	2.52429E-01	2.52272E-01	0.09	-0.062
	5,45,5	1.50260E-01	1.50171E-01	0.08	-0.059
3A	5,55,5	9.91726E-02	9.91150E-02	0.08	-0.058
	5,65,5	4.22623E-02	4.22382E-02	0.07	-0.057
	5,75,5	1.14703E-02	1.14638E-02	0.07	-0.057
	5,86,5	3.24662E-03	3.24482E-03	0.07	-0.055
	5,95,5	9.48324E-04	9.47802E-04	0.07	-0.055
	5,55,5	9.91726E-02	9.91150E-02	0.08	-0.058
	15,55,5	2.45041E-02	2.44840E-02	0.12	-0.082
	25,55,5	4.54477E-03	4.54047E-03	0.12	-0.095
3B	35,55,5	1.42960E-03	1.42832E-03	0.11	-0.090
	45,55,5	2.64846E-04	2.64613E-04	0.10	-0.088
	55,55,5	9.14210E-05	9.13463E-05	0.09	-0.082
	5,95,35	3.27058E-05	3.27271E-05	0.14	0.065
	15,95,35	2.68415E-05	2.68949E-05	0.15	0.199
	25,95,35	1.70019E-05	1.70202E-05	0.16	0.108
3C	35,95,35	3.37981E-05	3.37871E-05	0.15	-0.033
	45,95,35	6.04893E-06	6.03696E-06	0.14	-0.198
	55,95,35	3.36460E-06	3.36143E-06	0.09	-0.094

Table 2. Total flux for 50 % scattering cases

Case	Case ii (50% scattering)					
	Co-ordinates	GMVP		MCNP5		
	(cm)	Total Flux	FSD	Total Flux	FSD	Difference
	(x,y,z)	($cm^{-2}s^{-1}$)	1σ(%)	($cm^{-2}s^{-1}$)	1σ(%)	(%)
1A	5,5,5	8.29260E+00	0.021	8.22408E+00	0.02	-0.008
	5,15,5	1.87028E+00	0.005	1.87064E+00	0.02	0.000
	5,25,5	7.13986E-01	0.003	7.14038E-01	0.01	0.000
	5,35,5	3.84685E-01	0.004	3.84703E-01	0.01	0.000
	5,45,5	2.53984E-01	0.006	2.53979E-01	0.01	0.000
	5,55,5	1.37220E-01	0.073	1.37444E-01	0.05	0.002
	5,65,5	4.65913E-02	0.117	4.67619E-02	0.07	0.004
	5,75,5	1.58766E-02	0.197	1.59203E-02	0.08	0.003
	5,86,5	5.47036E-03	0.343	5.47819E-03	0.12	0.001
	5,95,5	1.85082E-03	0.619	1.83512E-03	0.19	-0.008
1B	5,5,5	8.29260E+00	0.021	8.22408E+00	0.02	-0.008
	15,15,15	6.63233E-01	0.004	6.63278E-01	0.01	0.000
	25,25,25	2.68828E-01	0.003	2.68827E-01	0.01	0.000
	35,35,35	1.56683E-01	0.005	1.56678E-01	0.01	0.000
	45,45,45	1.04405E-01	0.011	1.04421E-01	0.02	0.000
	55,55,55	3.02145E-02	0.061	2.99188E-02	0.09	-0.010
	65,65,65	4.06555E-03	0.074	4.05715E-03	0.15	-0.002
	75,75,75	5.86124E-04	0.116	5.88346E-04	0.34	0.004
	85,85,85	8.66059E-05	0.198	8.59860E-05	0.83	-0.007
	95,95,95	1.12892E-05	0.383	1.14439E-05	2.32	0.014
1C	5,55,5	1.37220E-01	0.073	1.37441E-01	0.36	0.002
	15,55,5	1.27890E-01	0.076	1.28225E-01	0.38	0.003
	25,55,5	1.13582E-01	0.080	1.13807E-01	0.39	0.002
	35,55,5	9.59578E-02	0.088	9.61031E-02	0.42	0.002
	45,55,5	7.82701E-02	0.094	7.78195E-02	0.45	-0.006
	55,55,5	5.67030E-02	0.111	5.59954E-02	0.50	-0.012
	65,55,5	1.88631E-02	0.189	1.87846E-02	0.64	-0.004
	75,55,5	6.46624E-03	0.314	6.53919E-03	0.86	0.011
	85,55,5	2.28099E-03	0.529	2.29033E-03	1.25	0.004
	95,55,5	7.93924E-04	0.890	8.17436E-04	2.05	0.030
2A	5,5,5	8.61696E+00	0.063	8.54827E+00	0.08	-0.008
	5,15,5	2.16123E+00	0.015	2.15974E+00	0.05	-0.001
	5,25,5	8.93437E-01	0.011	8.93124E-01	0.05	0.000
	5,35,5	4.77452E-01	0.012	4.77515E-01	0.06	0.000
	5,45,5	2.88719E-01	0.013	2.88702E-01	0.07	0.000
	5,55,5	1.88959E-01	0.014	1.88887E-01	0.08	0.000
	5,65,5	1.31026E-01	0.016	1.31016E-01	0.09	0.000
	5,75,5	9.49890E-02	0.017	9.49280E-02	0.10	-0.001
	5,86,5	7.12403E-02	0.019	7.12383E-02	0.11	0.000
	5,95,5	5.44807E-02	0.019	5.44765E-02	0.11	0.000

	5,95,5	5.44807E-02	0.019	5.44765E-02	0.11	0.000
	15,95,5	6.58233E-03	0.244	6.92456E-03	0.12	0.052
	25,95,5	1.28002E-03	0.336	1.30660E-03	0.11	0.021
2B	35,95,5	4.13414E-04	0.363	4.22438E-04	0.14	0.022
	45,95,5	1.55548E-04	0.454	1.57652E-04	0.19	0.014
	55,95,5	6.02771E-05	0.599	6.10116E-05	0.27	0.012
	5,5,5	8.61578E+00	0.044	8.55184E+00	0.06	-0.007
	5,15,5	2.16130E+00	0.010	2.16148E+00	0.04	0.000
	5,25,5	8.93784E-01	0.008	8.93860E-01	0.01	0.000
	5,35,5	4.78052E-01	0.008	4.78105E-01	0.02	0.000
	5,45,5	2.89424E-01	0.009	2.89449E-01	0.02	0.000
3A	5,55,5	1.92698E-01	0.010	1.92725E-01	0.02	0.000
	5,65,5	1.04982E-01	0.077	1.05339E-01	0.16	0.003
	5,75,5	3.37544E-02	0.107	3.38300E-02	0.23	0.002
	5,86,5	1.08158E-02	0.163	1.08253E-02	0.26	0.001
	5,95,5	3.39632E-03	0.275	3.39693E-03	0.30	0.000
	5,55,5	1.92698E-01	0.010	1.92725E-01	0.02	0.000
	15,55,5	6.72147E-02	0.019	6.72164E-02	0.08	0.000
	25,55,5	2.21799E-02	0.028	2.21903E-02	0.13	0.000
3B	35,55,5	9.90646E-03	0.033	9.91433E-03	0.17	0.001
	45,55,5	3.39066E-03	0.195	3.41643E-03	0.62	0.008
	55,55,5	1.05629E-03	0.327	1.06109E-03	0.58	0.005
	5,95,35	3.44804E-04	0.793	3.48081E-04	0.36	0.010
	15,95,35	2.91825E-04	0.659	2.88880E-04	0.40	-0.010
	25,95,35	2.05793E-04	0.529	2.06733E-04	0.62	0.005
3C	35,95,35	2.62086E-04	0.075	2.62612E-04	0.36	0.002
	45,95,35	1.05367E-04	0.402	1.07630E-04	1.68	0.021
	55,95,35	4.44962E-05	0.440	4.49852E-05	1.27	0.011

Figure 1. Relative flux of problem 1Ai (x = z = 5 cm)

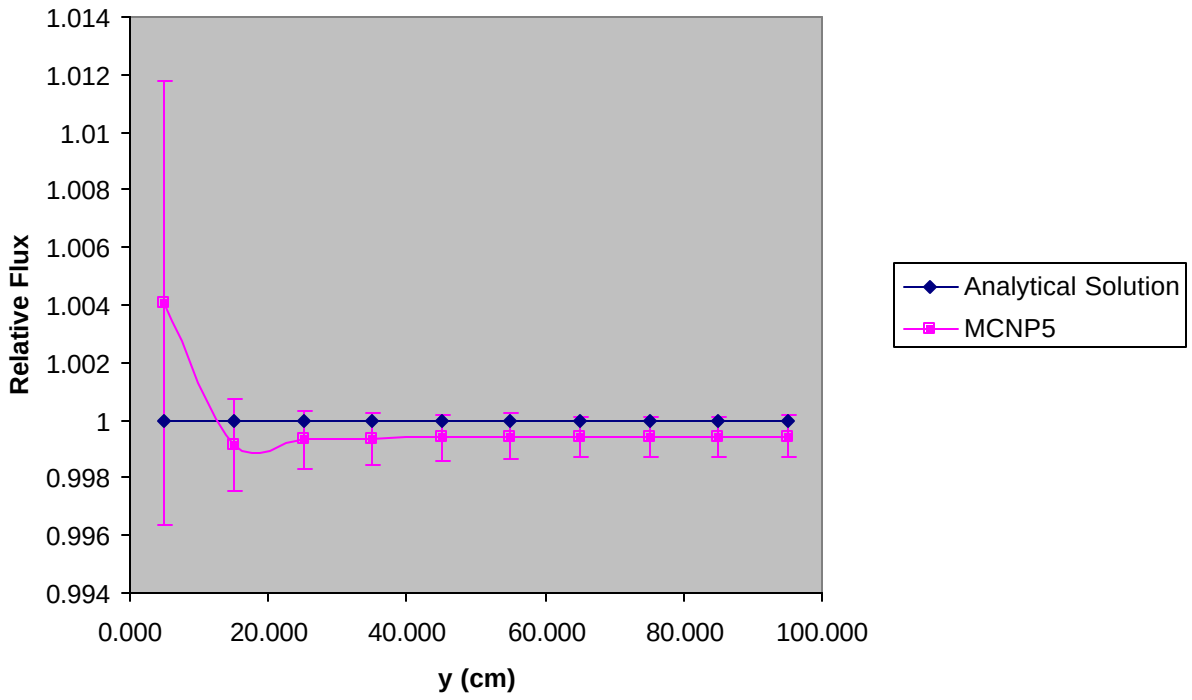

Figure 2. Relative flux of problem 1Aii (x = z = 5 cm)

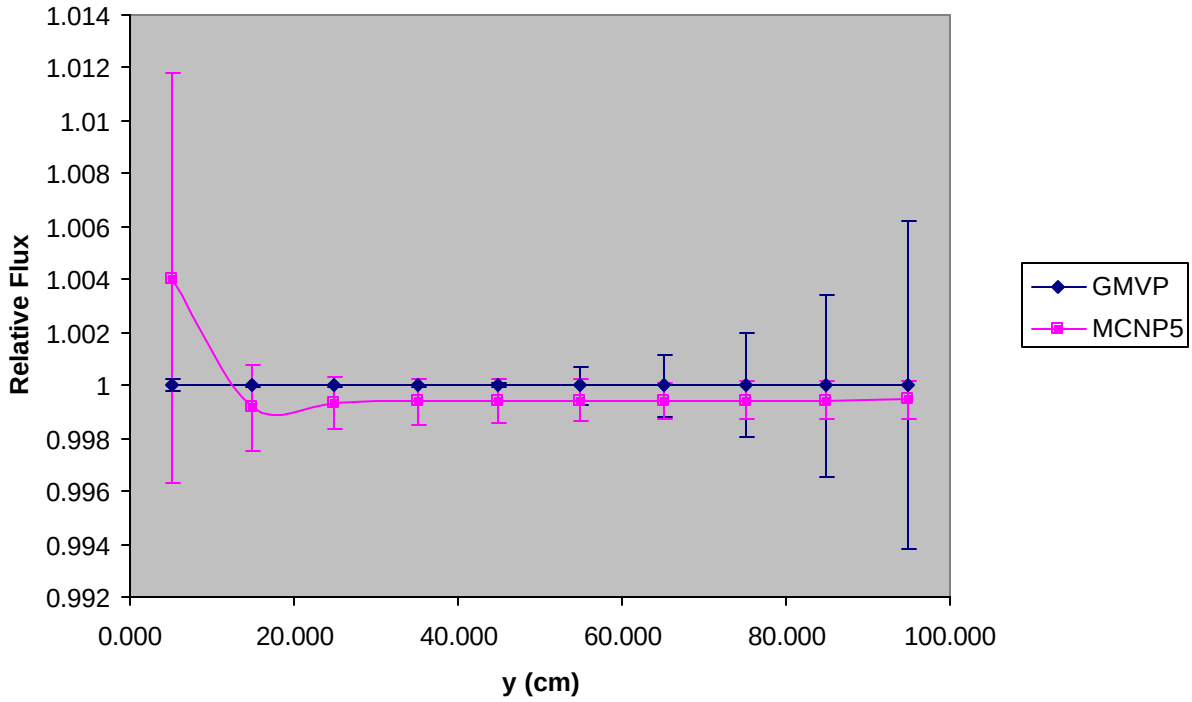

Figure 3. Relative flux of problem 1Bi (x = y = z)

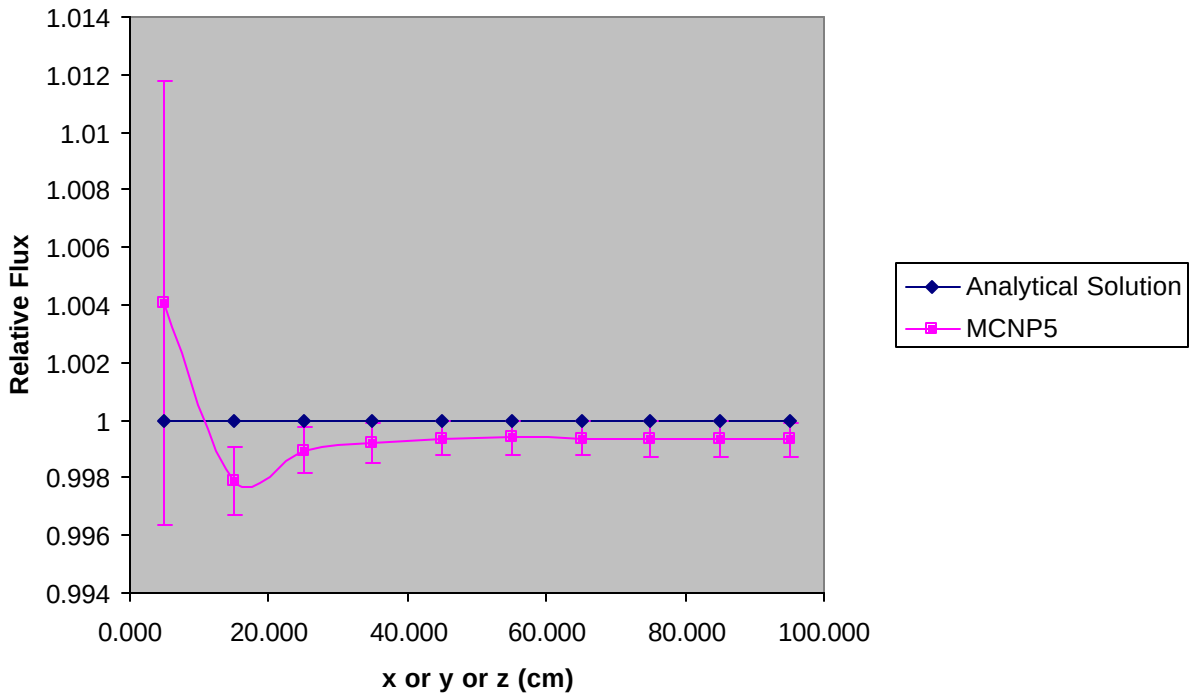

Figure 4. Relative flux of problem 1Bii (x = y = z)

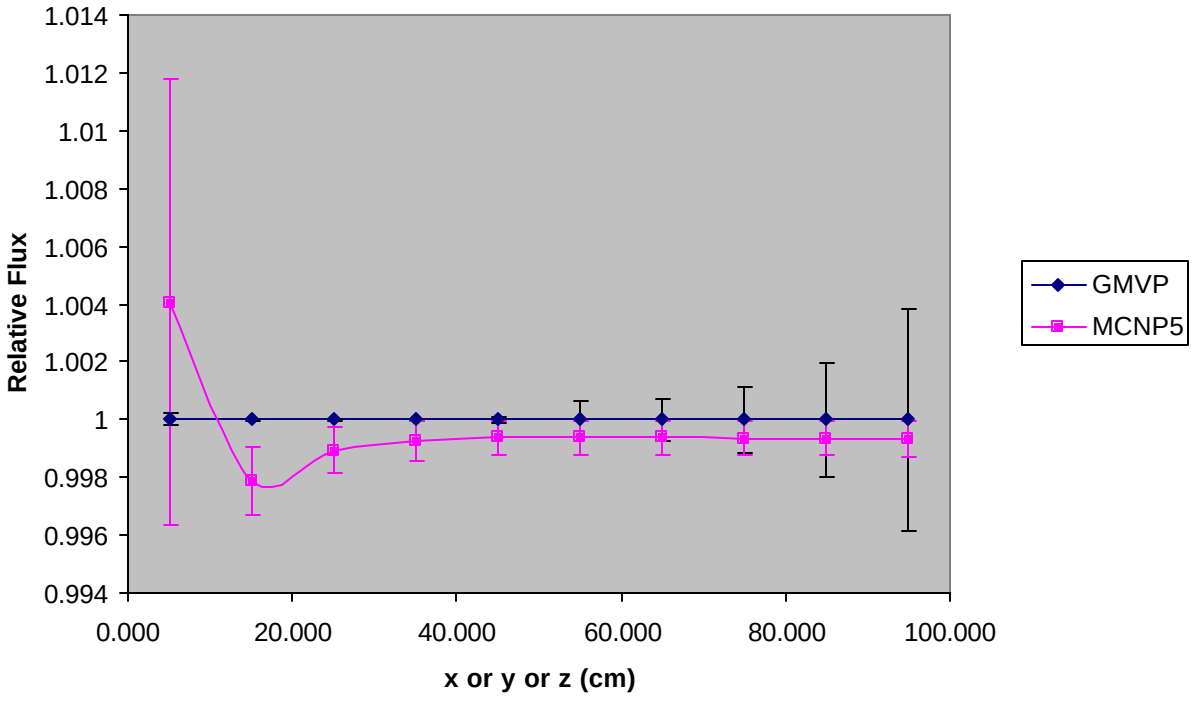

Figure 5. Relative flux of problem 1Ci (y = 55 cm, z = 5 cm)

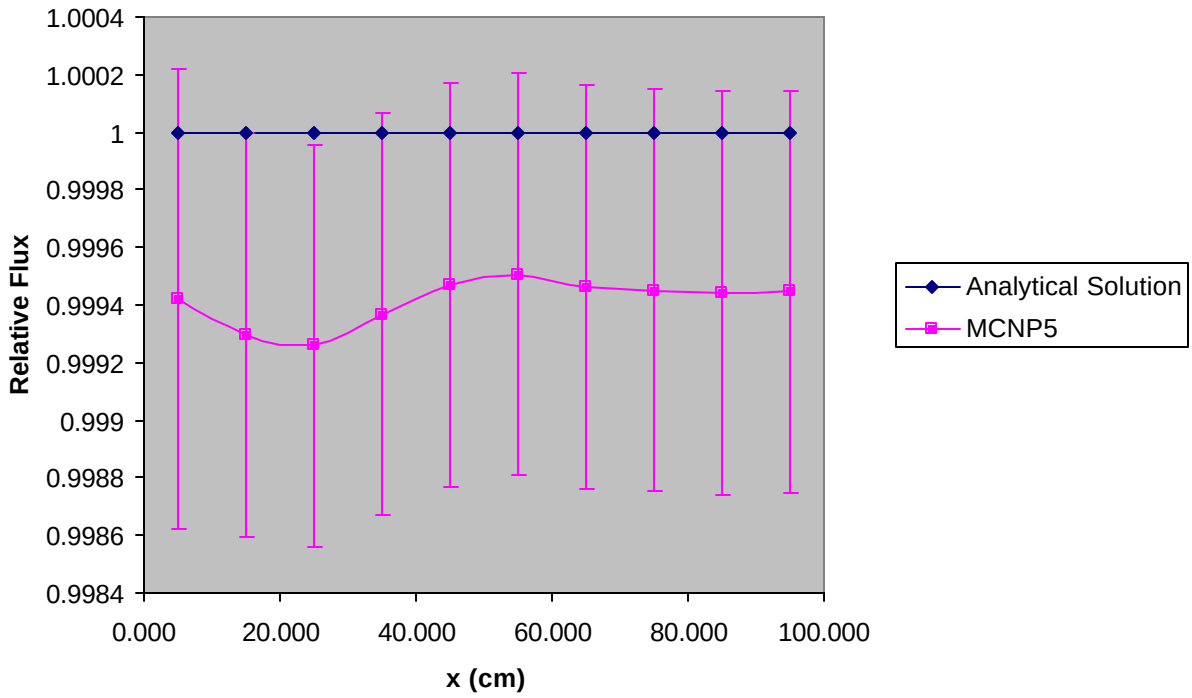

Figure 6. Relative flux of problem 1Cii (y = 55 cm, z = 5 cm)

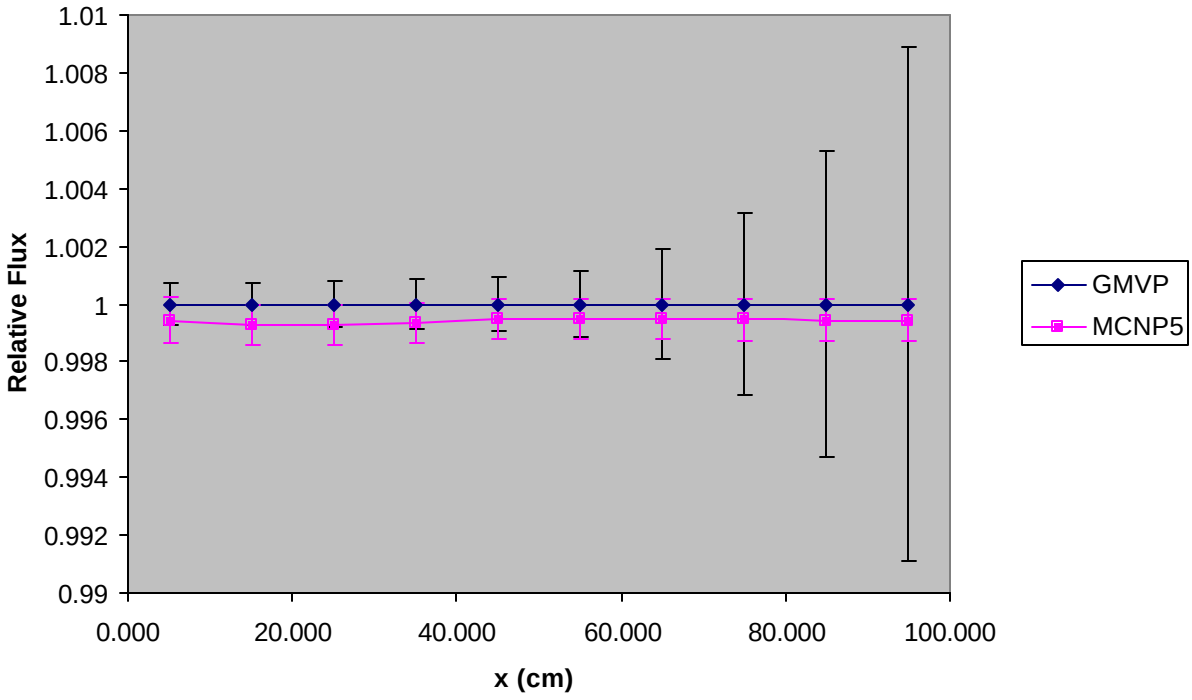

Figure 7. Relative flux of problem 2Ai (x = z = 5 cm)

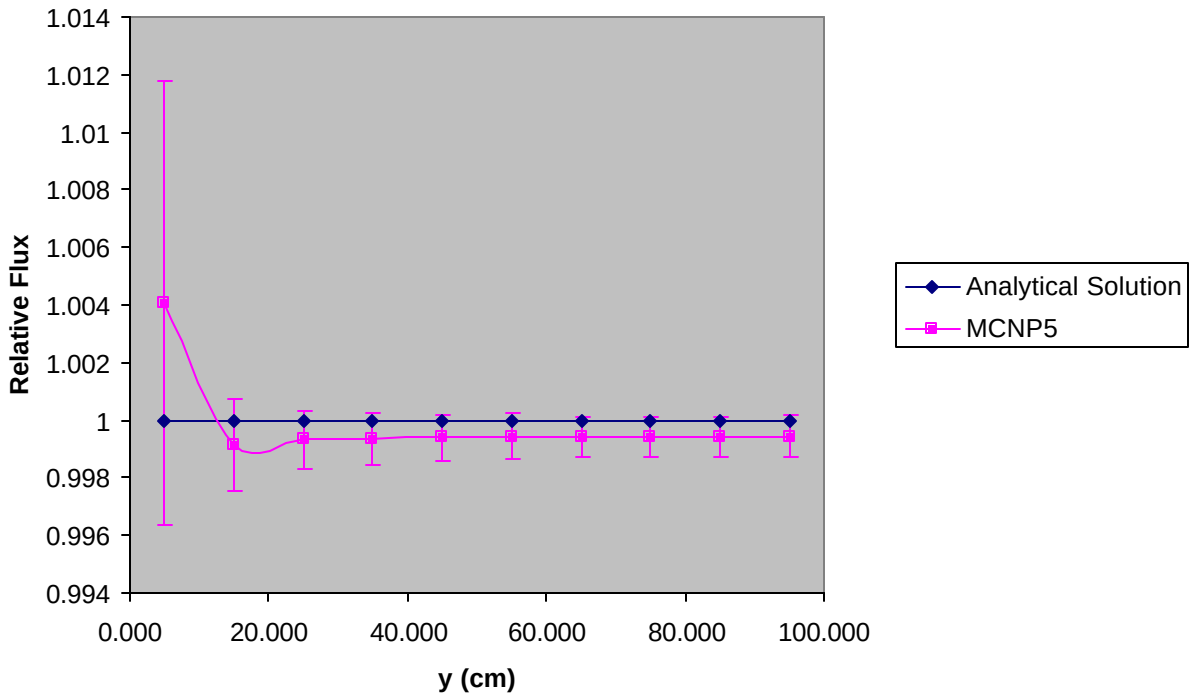

Figure 8. Relative flux of problem 2Aii (x = z = 5 cm)

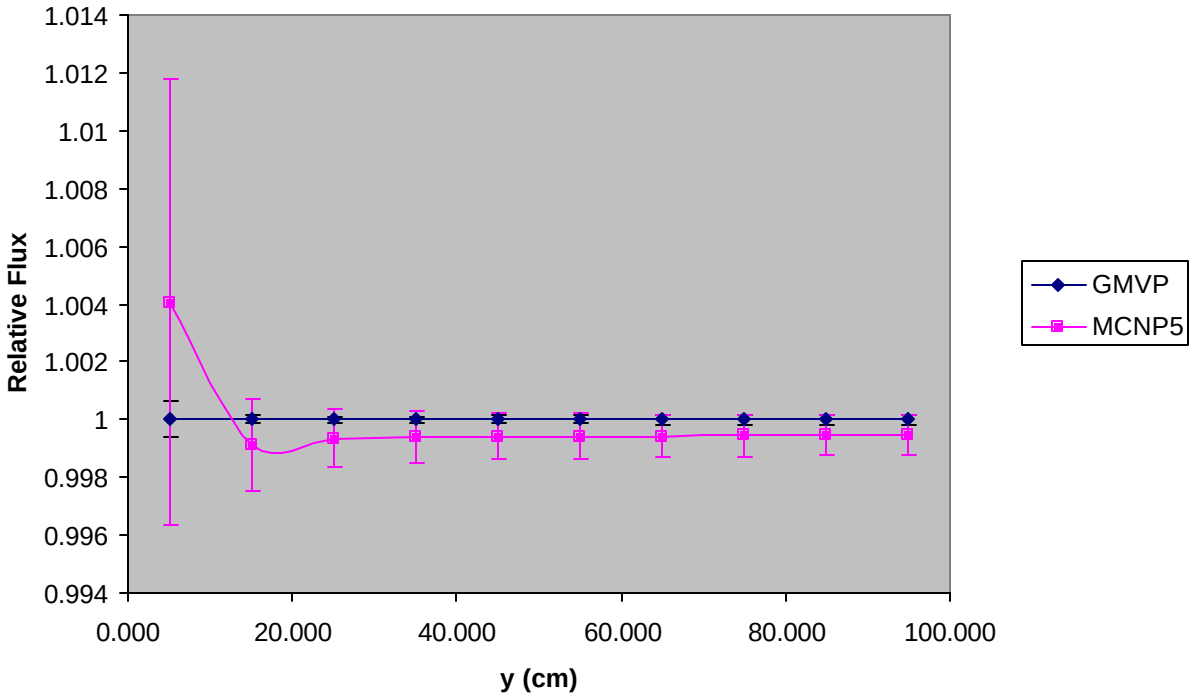

Figure 9. Relative flux of problem 2Bi (y = 95 cm, z = 5 cm)

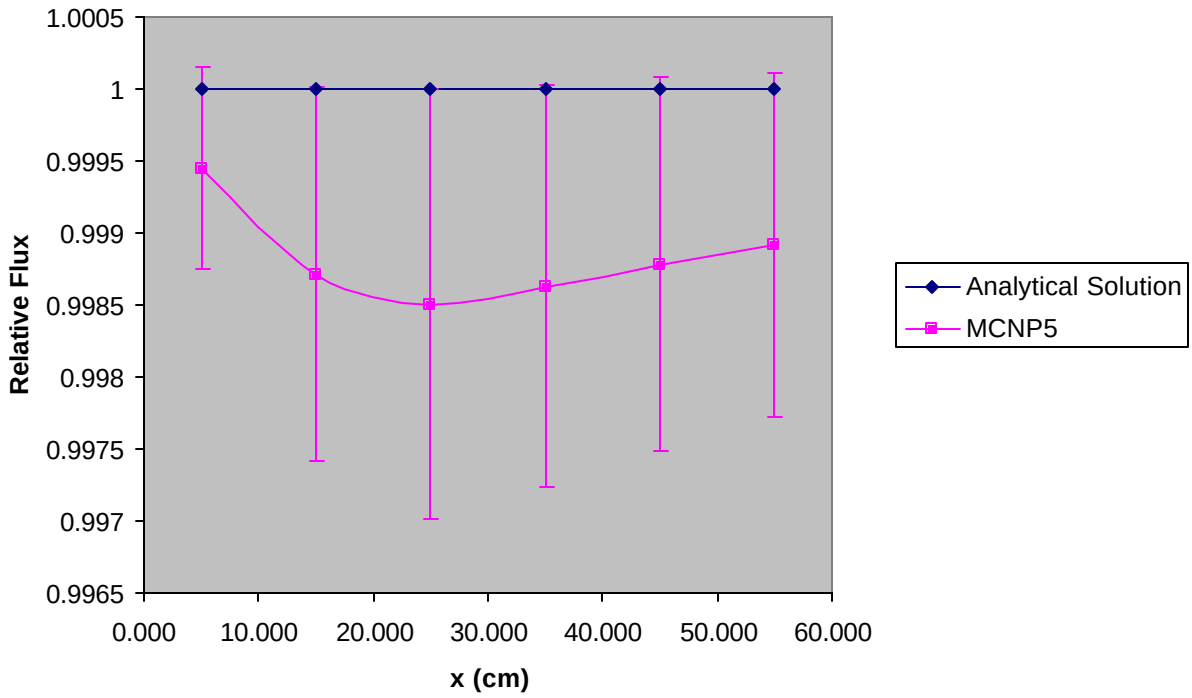

Figure 10. Relative flux of problem 2Bii (y = 95 cm, z = 5 cm)

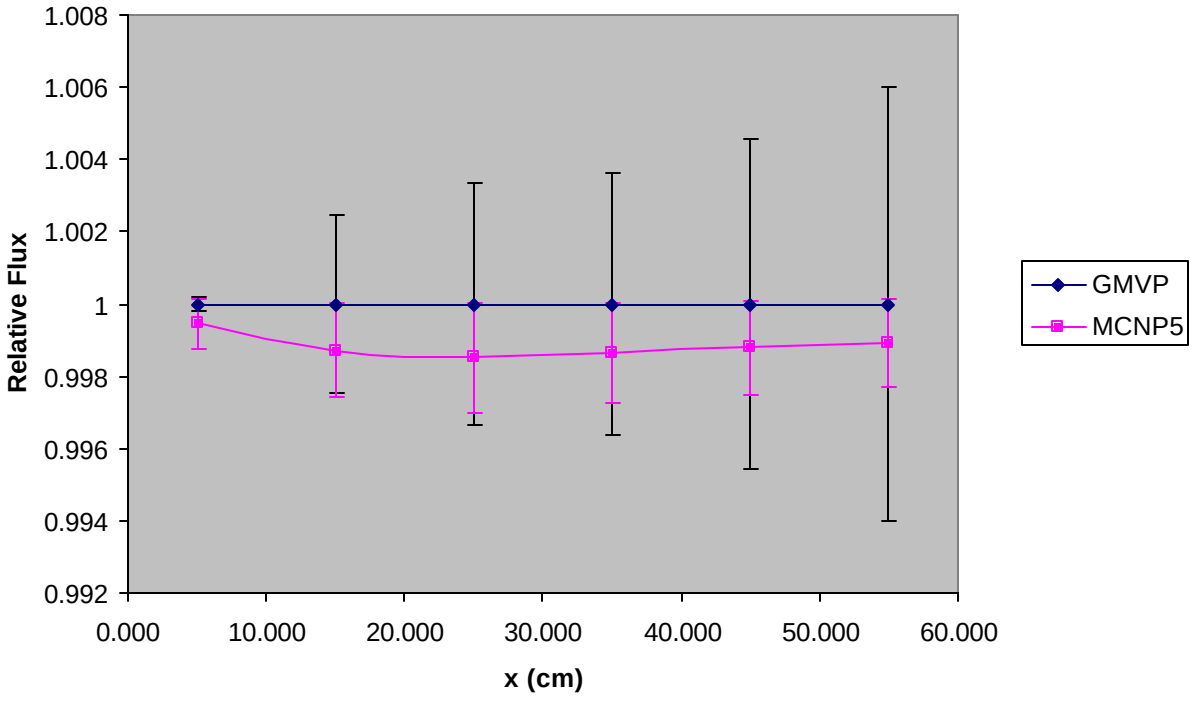

Figure 11. Relative flux of problem 3Ai (x = z = 5 cm)

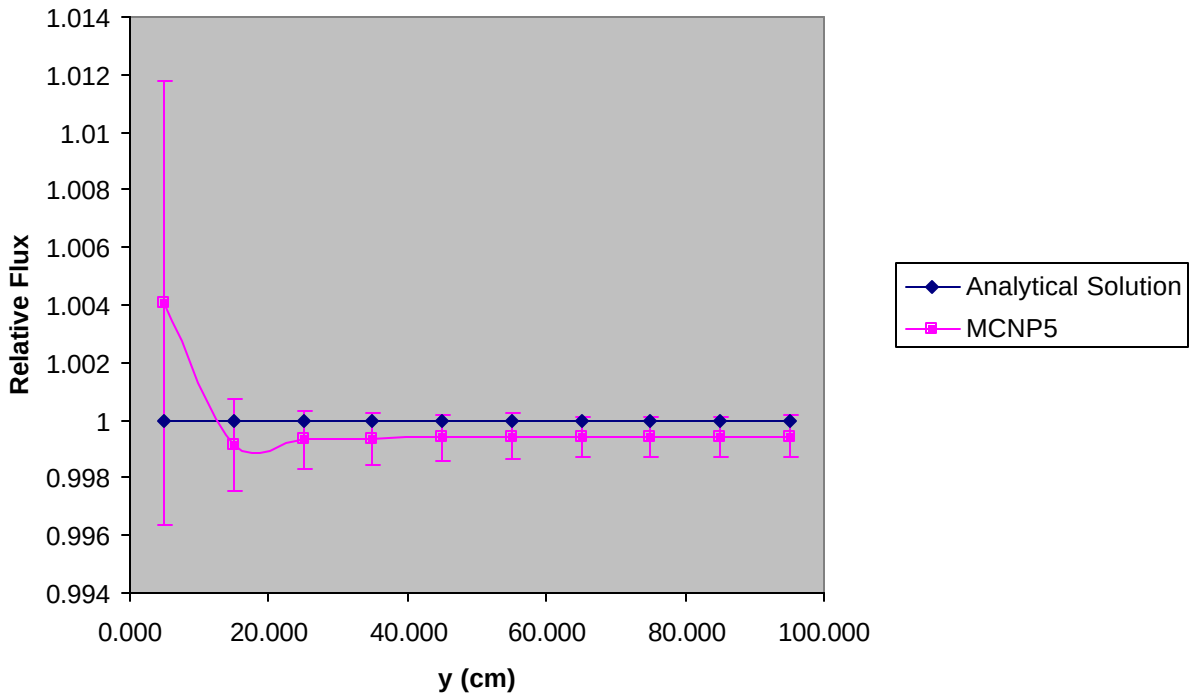

Figure 12. Relative flux of problem 3Aii (x = z = 5 cm)

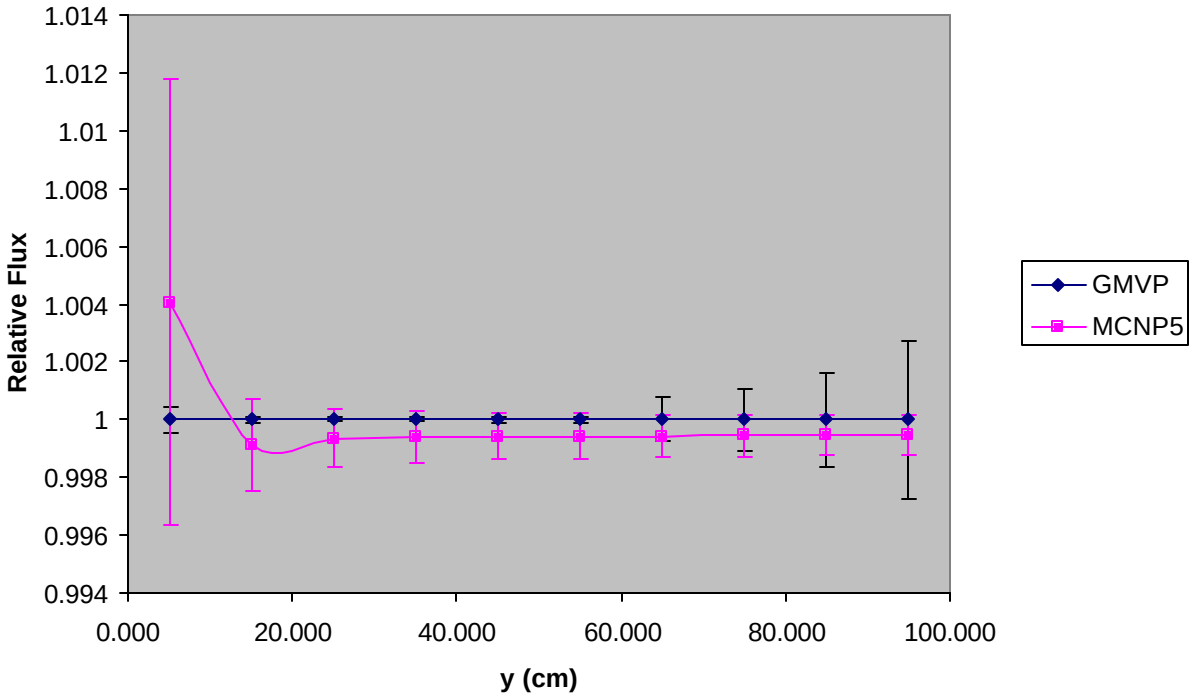

Figure 13. Relative flux of problem 3Bi (y = 55 cm, z = 5 cm)

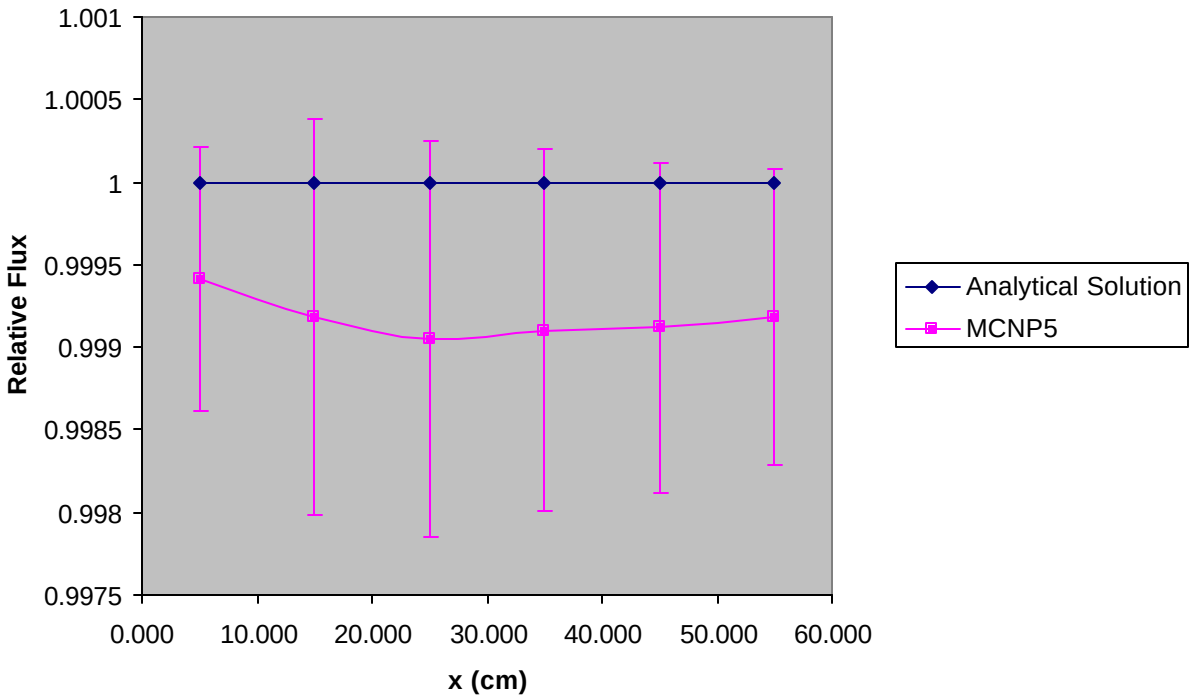

Figure 14. Relative flux of problem 3Bii (y = 55 cm, z = 5 cm)

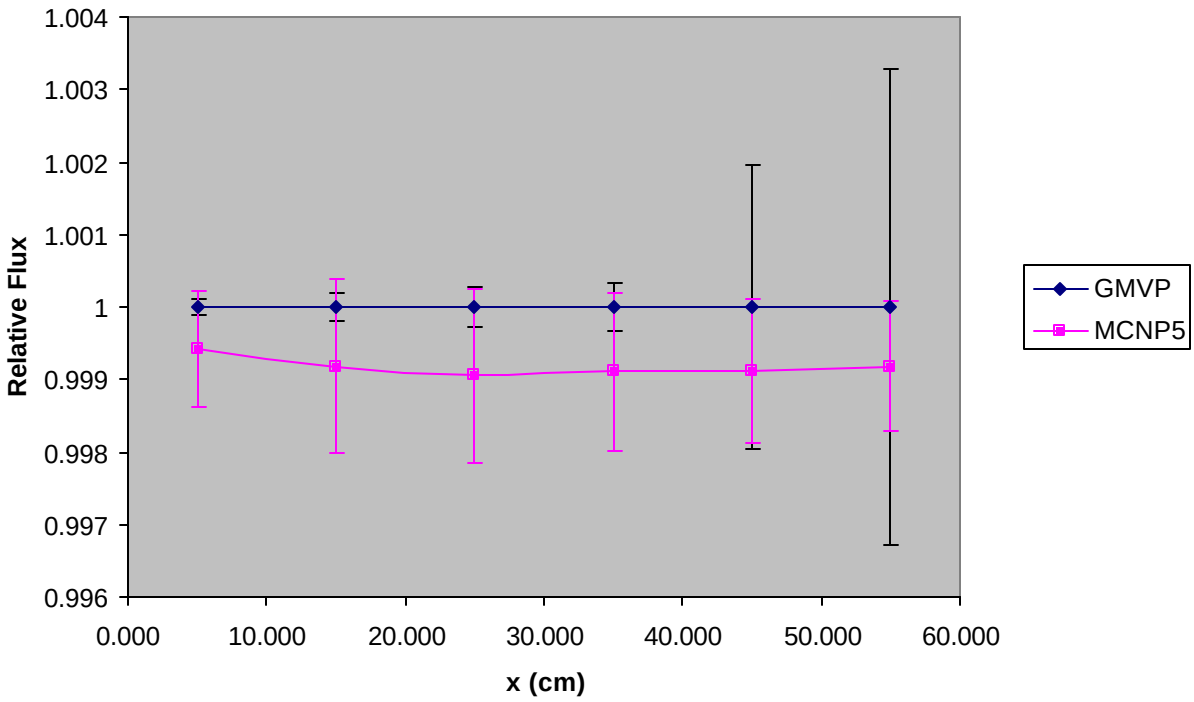

Figure 15. Relative flux of problem 3Ci (y =95 cm, z = 35 cm)

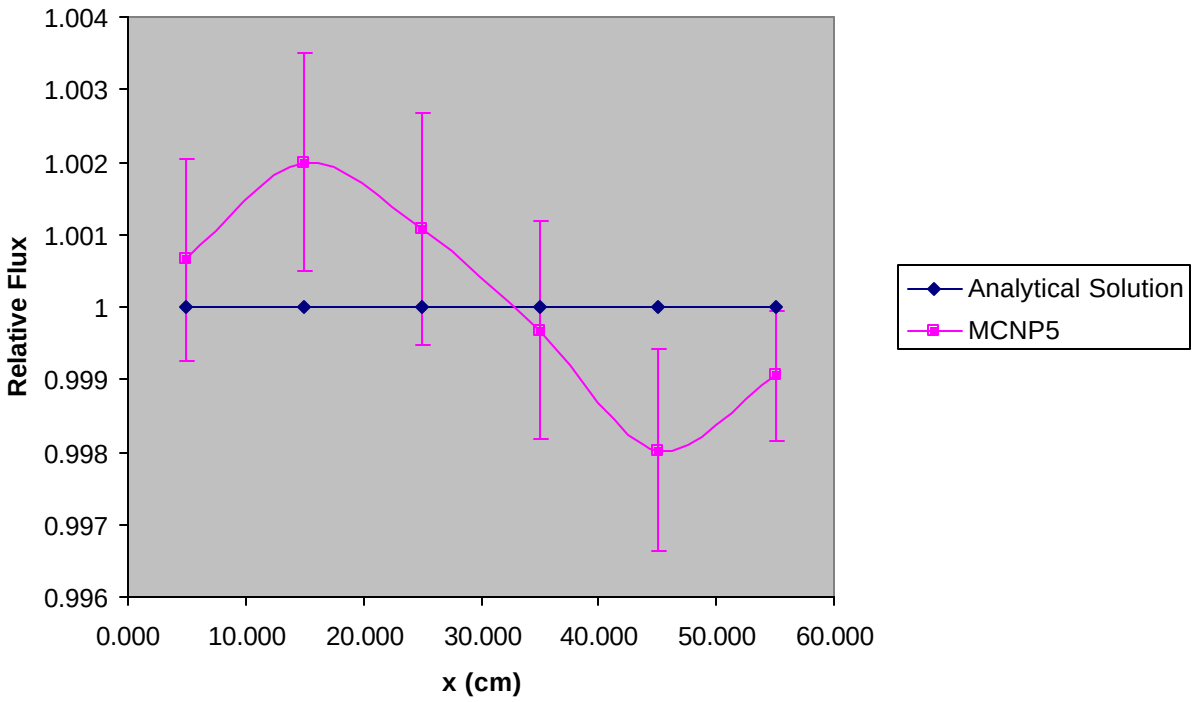

Figure 16. Relative flux of problem 3Cii (y = 95 cm, z = 35 cm)

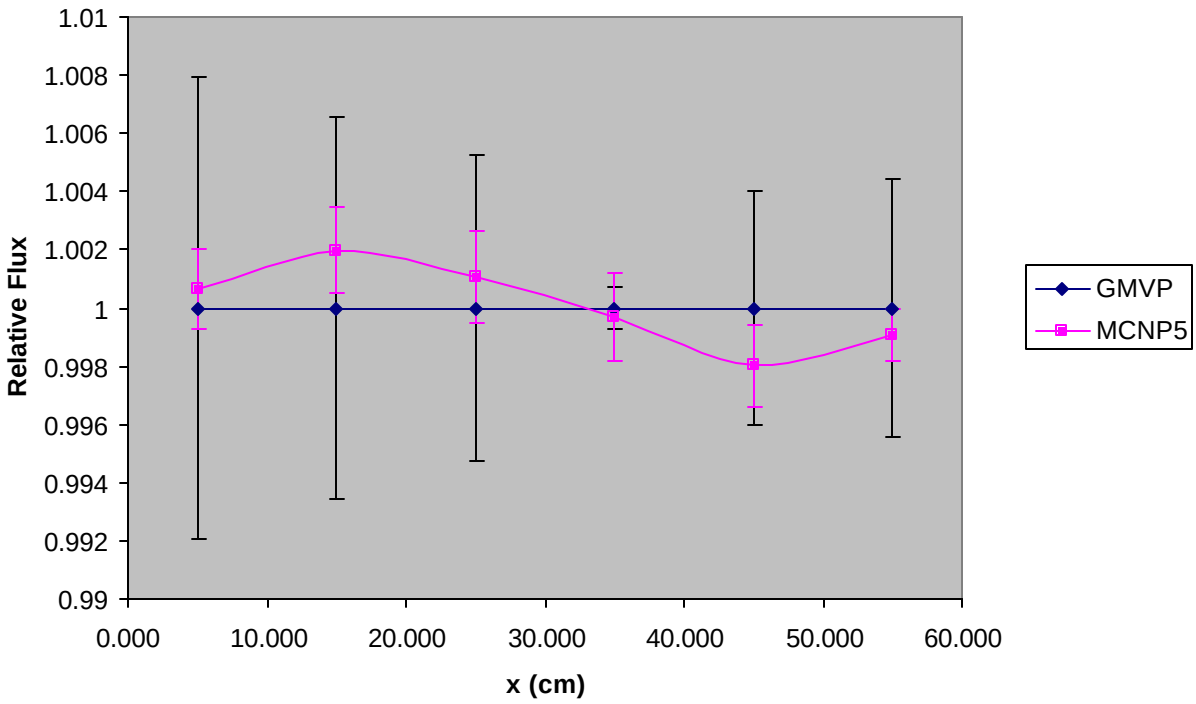

Discussion

A majority of the MCNP5 results matched, within one standard deviation, the values reported by Kobayashi. All results matched the Kobayashi data when quoted to two standard deviations. All of the MCNP5 results were within a half percent or less of the expected values. Much of the collected data appeared to trend below the expected fluxes; however, investigations showed that alteration of the random number generator seed would produce results that appeared to lie above the expected fluxes in addition to sets that would lie below the predicted fluxes. This demonstrated that an error, influencing the results to have a low trend, was not present in the code.

The results showed definite trends for a given random number seed for those portions of the problem where detectors were placed along a straight line from the origin. This can be seen in figures 1-4, 7-8, and 11-12. The random number generator caused this by propelling slightly fewer particles in the direction of the detectors. Particles that passed near a detector from the source would also pass near all those detectors on that line from the source. Conversely, when particles went in the opposite direction, none of the detectors on the line from the source would have significant scores from the particle.

Figures 15-16 show the most randomness because detectors in the 3C set were far from the source and were not along a line that passed through the source. A particle passing near one detector in the set would contribute a large score to that detector and comparatively smaller scores to the other detectors in the set. Figures 9-10 should also have demonstrated this randomness in the tallies; however, the nature of the straight duct, which transports most of the neutrons to the detectors in set 2B, caused less variation in the particle stream than the dogleg duct of problem 3. The 2B case also showed the low trend, possibly because the generator sent slightly more particles to the side of the geometry that was opposite of the detectors.

Another, less likely possibility for this low trend when comparing with the analytical solution could be that Kobayashi did not use the 10^{-4} cm^{-1} cross section for the void region. Instead, he may have simply used zero, which would account for the MCNP5 results being slightly lower than Kobayashi's analytical solutions. This is a concern because Kobayashi does not explicitly explain how he obtained his results in reference 1.

Conclusion

The new version, MCNP5, is fully capable of handling flux calculations in geometries with void regions, using the point detector estimator. The code is accurate for interfaces between highly absorbing media and void regions in addition to interfaces between scattering and void regions. The MCNP point detector estimators are capable of accurately determining neutron fluxes and satisfying statistical checks when the exclusion radii are on the order of one mean free path of neutrons in the medium.

References

[1] K. Kobayashi, N. Sugimura, Y. Nagaya, "3-D Radiation Transport Benchmark Problems and Results for Simple Geometries with Void Regions", OECD/NEA (2000).

[2] R.T. Ackroyd, N.S. Riyait, "Iteration and Extrapolation Method for the Approximate Solution of the Even-Parity Transport Equation for Systems with Voids", *Ann. Nucl. Energy*, 16, 1 (1989).

[3] K. Kobayashi, "A Proposal for 3-D Radiation Transport Benchmarks for Simple Geometries with Void Region, 3-D Deterministic Radiation Transport Computer Programs", OECD Proceedings, p. 403 (1997).

[4] T. Mori and M. Nakagawa, "MVP/GMVP: General Purpose Monte Carlo Codes", JAERI-Data/Code 94-007 (1994) [in Japanese].

Appendix

Figure 17. x – z or y – z plane of problem 1, shield with square void

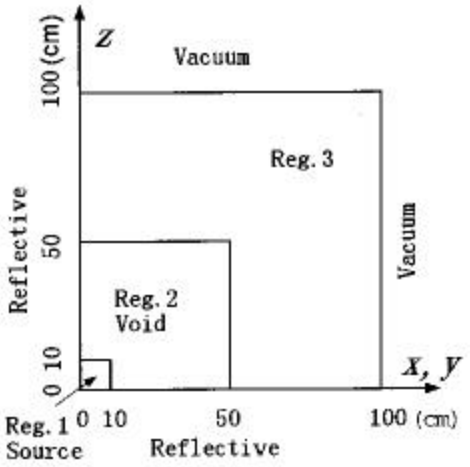

Figure 18. Sketch of problem 1, shield with square void

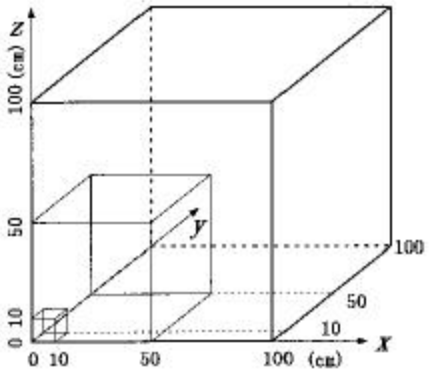

Figure 19. x – y or y – z plane of problem 2, shield with void duct

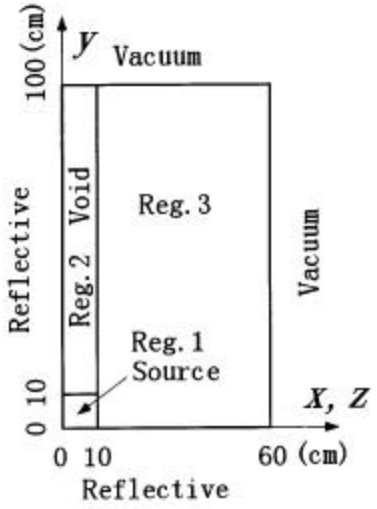

Figure 20. Sketch of problem 2, shield with void duct

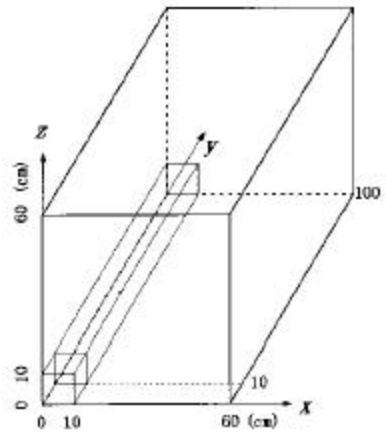

Figure 21. x – y plane of problem 3, shield with dog leg void duct

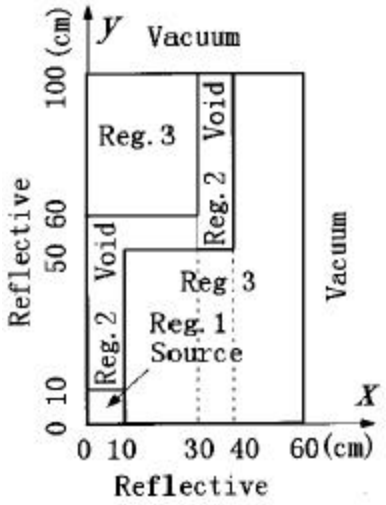

Figure 22. y – z plane of problem 3, shield with dog leg void duct

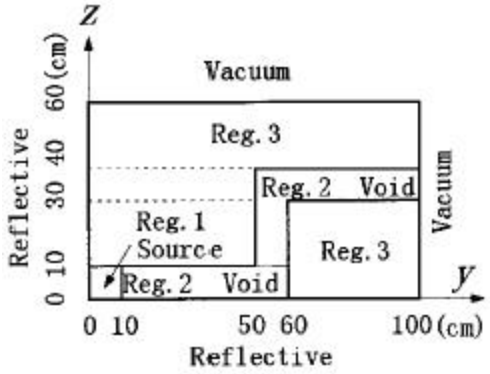

Figure 23. x – z plane of problem 3, shield with dog leg void duct

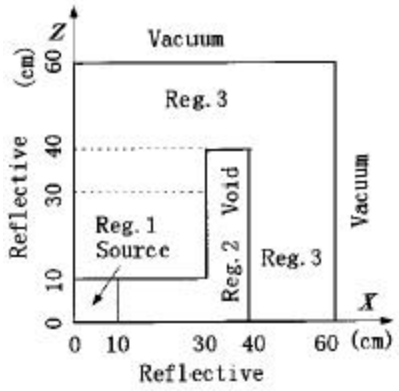

Figure 24. Sketch of problem 3, shield with dog leg void duct

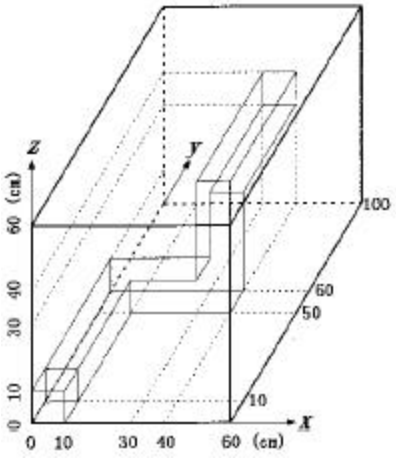

Input Files

‘p1ia’

```
Prob1 - OECD Benchmarks, 3D with voids
c
1 1 .1    -1
2 1 .0001  1 -2
3 1 .1     2 -3
4 0        3

1   rpp  -10.  10.  -10.  10.  -10.  10.
2   rpp  -50.  50.  -50.  50.  -50.  50.
3   rpp -100. 100. -100. 100. -100. 100.

nps  1000000
rand gen=2 seed=13
imp:n  1 1 1 0
sdef wgt=8000. x=d1 y=d2 z=d3
si1  -10. 10.
sp1  0  1
si2  -10. 10.
sp2  0  1
si3  -10. 10.
sp3  0  1
mgopt f 1 0
m1 99001.00m 1.
print
c
f005:n   5.  5.  5. 1
f015:n   5. 15.  5. .01
f025:n   5. 25.  5. .01
f035:n   5. 35.  5. .01
f045:n   5. 45.  5. .01
f055:n   5. 55.  5. .01
f065:n   5. 65.  5. .01
f075:n   5. 75.  5. .01
f085:n   5. 85.  5. .01
f095:n   5. 95.  5. .01
c
f115:n  15. 15. 15. .01
f125:n  25. 25. 25. .01
f135:n  35. 35. 35. .01
f145:n  45. 45. 45. .01
f155:n  55. 55. 55. .01
f165:n  65. 65. 65. .01
f175:n  75. 75. 75. .01
f185:n  85. 85. 85. .01
f195:n  95. 95. 95. .01
```

‘p1ib’

```
Prob1 - OECD Benchmarks, 3D with voids
c
1 1 .1    -1
2 1 .0001  1 -2
3 1 .1     2 -3
4 0        3

1   rpp  -10.  10.  -10.  10.  -10.  10.
2   rpp  -50.  50.  -50.  50.  -50.  50.
3   rpp -100. 100. -100. 100. -100. 100.

nps  1000000
rand gen=2 seed=13
imp:n  1 1 1 0
sdef wgt=8000. x=d1 y=d2 z=d3
si1  -10. 10.
sp1  0  1
si2  -10. 10.
sp2  0  1
si3  -10. 10.
sp3  0  1
mgopt f 1 0
m1 99001.00m 1.
print
c
f205:n   5. 55.  5. .01
f215:n  15. 55.  5. .01
f225:n  25. 55.  5. .01
f235:n  35. 55.  5. .01
f245:n  45. 55.  5. .01
f255:n  55. 55.  5. .01
f265:n  65. 55.  5. .01
f275:n  75. 55.  5. .01
f285:n  85. 55.  5. .01
f295:n  95. 55.  5. .01
```

‘p1iia’

```
Prob1 - OECD Benchmarks, 3D with voids and scattering
c
1 1 .1    -1
2 1 .0001  1 -2
3 1 .1     2 -3
4 0        3

1   rpp  -10.  10.  -10.  10.  -10.  10.
2   rpp  -50.  50.  -50.  50.  -50.  50.
4   rpp -100. 100. -100. 100. -100. 100.

nps  1e8
rand gen=2 seed=13
imp:n  1 2 16 0
sdef wgt=8000. x=d1 y=d2 z=d3
si1  -10. 10.
sp1  0  1
si2  -10. 10.
sp2  0  1
si3  -10. 10.
sp3  0  1
mgopt f 1 0
m1 99002.00m 1.
print
c
f005:n   5.  5.  5. 5
f015:n   5. 15.  5. 5
f025:n   5. 25.  5. 5
f035:n   5. 35.  5. 5
f045:n   5. 45.  5. 5
f055:n   5. 55.  5. 5
f065:n   5. 65.  5. 5
f075:n   5. 75.  5. 5
f085:n   5. 85.  5. 5
f095:n   5. 95.  5. 5
c
f115:n  15. 15. 15. 5
f125:n  25. 25. 25. 5
f135:n  35. 35. 35. 5
f145:n  45. 45. 45. 5
f155:n  55. 55. 55. 5
f165:n  65. 65. 65. 5
f175:n  75. 75. 75. 5
f185:n  85. 85. 85. 5
f195:n  95. 95. 95. 5
```

‘p1iib’

```
Prob1 - OECD Benchmarks, 3D with voids and scattering
c
1 1 .1    -1
2 1 .0001  1 -2
3 1 .1     2 -3
4 0        3

1   rpp  -10.  10.  -10.  10.  -10.  10.
2   rpp  -50.  50.  -50.  50.  -50.  50.
3   rpp -100. 100. -100. 100. -100. 100.

nps  2e8
rand gen=2 seed=13
imp:n  1 2 8m 0
sdef wgt=8000. x=d1 y=d2 z=d3
si1  -10. 10.
sp1  0  1
si2  -10. 10.
sp2  0  1
si3  -10. 10.
sp3  0  1
mgopt f 1 0
m1 99002.00m 1.
print
c
f205:n   5. 55.  5. 5
f215:n  15. 55.  5. 5
f225:n  25. 55.  5. 5
f235:n  35. 55.  5. 5
f245:n  45. 55.  5. 5
f255:n  55. 55.  5. 5
f265:n  65. 55.  5. 5
f275:n  75. 55.  5. 5
f285:n  85. 55.  5. 5
f295:n  95. 55.  5. 5
```

‘p2ia’

```
Prob2 - OECD Benchmarks, 3D with voids
c
1 1 .1    -1
2 1 .0001  1 -2
3 1 .1     2 -3
4 0        3

1   rpp  -10.  10.  -10.  10.  -10.  10.
2   rpp  -10.  10. -100. 100.  -10.  10.
3   rpp  -60.  60. -100. 100.  -60.  60.

nps  1000000
rand gen=2 seed=13
imp:n  1 1 1 0
sdef wgt=8000. x=d1 y=d2 z=d3
si1  -10. 10.
sp1  0  1
si2  -10. 10.
sp2  0  1
si3  -10. 10.
sp3  0  1
mgopt f 1 0
m1 99001.00m 1.
print
c
f005:n   5.  5.  5. 1
f015:n   5. 15.  5. .01
f025:n   5. 25.  5. .01
f035:n   5. 35.  5. .01
f045:n   5. 45.  5. .01
f055:n   5. 55.  5. .01
f065:n   5. 65.  5. .01
f075:n   5. 75.  5. .01
f085:n   5. 85.  5. .01
f095:n   5. 95.  5. .01
c
f105:n   5. 95.  5. .01
f115:n  15. 95.  5. .01
f125:n  25. 95.  5. .01
f135:n  35. 95.  5. .01
f145:n  45. 95.  5. .01
f155:n  55. 95.  5. .01
```

‘p2iia’

```
Prob2 OECD Benchmarks - Voids with scattering
1 1 .1    -1
2 1 .0001  1 -2
3 1 .1     2 -3
4 1 .1     2 3 -4
5 0        4

1   rpp  -10.  10.  -10.  10.  -10.  10.
2   rpp  -10.  10. -100. 100.  -10.  10.
3   rpp  -40.  40. -80.   80.  -40.  40.
4   rpp  -60.  60. -100. 100.  -60.  60.

nps  200000000
imp:n  1 4m 8m 8m 0
sdef wgt=8000. x=d1 y=d2 z=d3
si1  -10. 10.
sp1  0  1
si2  -10. 10.
sp2  0  1
si3  -10. 10.
sp3  0  1
mgopt f 1 0
m1 99002.00m 1.
print
c
f005:n   5.  5.  5. 5
f015:n   5. 15.  5. 5
f025:n   5. 25.  5. 5
f035:n   5. 35.  5. 5
f045:n   5. 45.  5. 5
f055:n   5. 55.  5. 5
f065:n   5. 65.  5. 5
f075:n   5. 75.  5. 5
f085:n   5. 85.  5. 5
f095:n   5. 95.  5. 5
c
f105:n   5. 95.  5. 5
f115:n  15. 95.  5. 5
f125:n  25. 95.  5. 5
f135:n  35. 95.  5. 5
f145:n  45. 95.  5. 5
f155:n  55. 95.  5. 5
```

‘p3ia’

```
Prob3 - OECD Benchmarks, 3D with voids
1 1 .1    -100
2 1 .0001 -201 : -202 : -203 : -204 : -205 : -206 : -207 : -208 :
          -209 : -210 : -211 : -212 : -213 : -214 : -215 : -216
3 1 .1     #1 #2 -300
4 0        300

100 rpp  -10.  10.  -10.   10.  -10.  10.
201 rpp  -10.  10.   10.   50.  -10.  10.
202 rpp  -10.  10.  -50.  -10.  -10.  10.
203 rpp  -30.  30.   50.   60.  -10.  10.
204 rpp  -30.  30.  -60.  -50.  -10.  10.
205 rpp   30.  40.   50.   60.  -30.  30.
206 rpp  -40. -30.   50.   60.  -30.  30.
207 rpp   30.  40.  -60.  -50.  -30.  30.
208 rpp  -40. -30.  -60.  -50.  -30.  30.
209 rpp   30.  40.   50.  100.   30.  40.
210 rpp   30.  40. -100.  -50.   30.  40.
211 rpp   30.  40.   50.  100.  -40. -30.
212 rpp   30.  40. -100.  -50.  -40. -30.
213 rpp  -40. -30.   50.  100.   30.  40.
214 rpp  -40. -30. -100.  -50.   30.  40.
215 rpp  -40. -30.   50.  100.  -40. -30.
216 rpp  -40. -30. -100.  -50.  -40. -30.
300 rpp  -60.  60. -100.  100.  -60.  60.

nps  1000000
rand gen=2 seed=13
imp:n  1 1 1 0
sdef wgt=8000. x=d1 y=d2 z=d3
si1  -10. 10.
sp1  0  1
si2  -10. 10.
sp2  0  1
si3  -10. 10.
sp3  0  1
mgopt f 1 0
m1 99001.00m 1.
print
f005:n   5.  5.  5. 1
f015:n   5. 15.  5. .01
f025:n   5. 25.  5. .01
f035:n   5. 35.  5. .01
f045:n   5. 45.  5. .01
f055:n   5. 55.  5. .01
f065:n   5. 65.  5. .01
f075:n   5. 75.  5. .01
f085:n   5. 85.  5. .01
f095:n   5. 95.  5. .01
f105:n   5. 55.  5. .01
f115:n  15. 55.  5. .01
f125:n  25. 55.  5. .01
f135:n  35. 55.  5. .01
f145:n  45. 55.  5. .01
f155:n  55. 55.  5. .01
```

‘p3ib’

```
Prob3 - OECD Benchmarks, 3D with voids
c
1 1 .1    -100
2 1 .0001 -201 : -202 : -203 : -204 : -205 :
          -206 : -207 : -208 : -209 : -210 :
          -211 : -212 : -213 : -214 : -215 :
          -216
3 1 .1     #1 #2 -300
4 0        300

100 rpp  -10.  10.  -10.   10.  -10.  10.
c   -----------------------------------
201 rpp  -10.  10.   10.   50.  -10.  10.
202 rpp  -10.  10.  -50.  -10.  -10.  10.
c   -----------------------------------
203 rpp  -30.  30.   50.   60.  -10.  10.
204 rpp  -30.  30.  -60.  -50.  -10.  10.
c   -----------------------------------
205 rpp   30.  40.   50.   60.  -30.  30.
206 rpp  -40. -30.   50.   60.  -30.  30.
207 rpp   30.  40.  -60.  -50.  -30.  30.
208 rpp  -40. -30.  -60.  -50.  -30.  30.
c   -----------------------------------
209 rpp   30.  40.   50.  100.   30.  40.
210 rpp   30.  40. -100.  -50.   30.  40.
211 rpp   30.  40.   50.  100.  -40. -30.
212 rpp   30.  40. -100.  -50.  -40. -30.
213 rpp  -40. -30.   50.  100.   30.  40.
214 rpp  -40. -30. -100.  -50.   30.  40.
215 rpp  -40. -30.   50.  100.  -40. -30.
216 rpp  -40. -30. -100.  -50.  -40. -30.
c   -----------------------------------
300 rpp  -60.  60. -100.  100.  -60.  60.

nps  1000000
rand gen=2 seed=13
imp:n  1 1 1 0
sdef wgt=8000. x=d1 y=d2 z=d3
si1  -10. 10.
sp1  0  1
si2  -10. 10.
sp2  0  1
si3  -10. 10.
sp3  0  1
mgopt f 1 0
m1 99001.00m 1.
print
f205:n   5. 95. 35. .01
f215:n  15. 95. 35. .01
f225:n  25. 95. 35. .01
f235:n  35. 95. 35. .01
f245:n  45. 95. 35. .01
f255:n  55. 95. 35. .01
```

‘p3iia’

```
Prob3 - OECD Benchmarks, 3D with voids and scattering
c
1 1 .1    -100
2 1 .0001 -201 : -202 : -203 : -204 : -205 : -206 : -207 : -208 :
          -209 : -210 : -211 : -212 : -213 : -214 : -215 : -216
3 1 .1     100 #2 -400
4 1 .1     209 210 211 212 213 214 215 216 400 -300
5 0        300

100 rpp  -10.  10.  -10.   10.  -10.  10.
201 rpp  -10.  10.   10.   50.  -10.  10.
202 rpp  -10.  10.  -50.  -10.  -10.  10.
203 rpp  -30.  30.   50.   60.  -10.  10.
204 rpp  -30.  30.  -60.  -50.  -10.  10.
205 rpp   30.  40.   50.   60.  -30.  30.
206 rpp  -40. -30.   50.   60.  -30.  30.
207 rpp   30.  40.  -60.  -50.  -30.  30.
208 rpp  -40. -30.  -60.  -50.  -30.  30.
209 rpp   30.  40.   50.  100.   30.  40.
210 rpp   30.  40. -100.  -50.   30.  40.
211 rpp   30.  40.   50.  100.  -40. -30.
212 rpp   30.  40. -100.  -50.  -40. -30.
213 rpp  -40. -30.   50.  100.   30.  40.
214 rpp  -40. -30. -100.  -50.   30.  40.
215 rpp  -40. -30.   50.  100.  -40. -30.
216 rpp  -40. -30. -100.  -50.  -40. -30.
300 rpp  -60.  60. -100.  100.  -60.  60.
400 rpp  -40.  40. -80.   80.   -40.  40.

nps  5e7
imp:n  1 1m 8m 10m 0
sdef wgt=8000. x=d1 y=d2 z=d3
si1  -10. 10.
sp1  0  1
si2  -10. 10.
sp2  0  1
si3  -10. 10.
sp3  0  1
mgopt f 1 0
m1 99002.00m 1.
print
f005:n   5.  5.  5. 5
f015:n   5. 15.  5. 5
f025:n   5. 25.  5. 5
f035:n   5. 35.  5. 5
f045:n   5. 45.  5. 5
f055:n   5. 55.  5. 5
f065:n   5. 65.  5. 5
f075:n   5. 75.  5. 5
f085:n   5. 85.  5. 5
f095:n   5. 95.  5. 5
f115:n  15. 55.  5. 5
f125:n  25. 55.  5. 5
f135:n  35. 55.  5. 5
f145:n  45. 55.  5. 5
f155:n  55. 55.  5. 5
```

‘p3iib’

```
Prob3 - OECD Benchmarks, 3D with voids and scattering
c
1 1 .1    -100
2 1 .0001 -201 : -202 : -203 : -204 : -205 :
          -206 : -207 : -208 : -209 : -210 :
          -211 : -212 : -213 : -214 : -215 :
          -216
3 1 .1     100 #2 -400
4 1 .1     209 210 211 212 213 214 215 216 400 -300
5 0        300

100 rpp  -10.  10.  -10.   10.  -10.  10.
c   -----------------------------------
201 rpp  -10.  10.   10.   50.  -10.  10.
202 rpp  -10.  10.  -50.  -10.  -10.  10.
c   -----------------------------------
203 rpp  -30.  30.   50.   60.  -10.  10.
204 rpp  -30.  30.  -60.  -50.  -10.  10.
c   -----------------------------------
205 rpp   30.  40.   50.   60.  -30.  30.
206 rpp  -40. -30.   50.   60.  -30.  30.
207 rpp   30.  40.  -60.  -50.  -30.  30.
208 rpp  -40. -30.  -60.  -50.  -30.  30.
c   -----------------------------------
209 rpp   30.  40.   50.  100.   30.  40.
210 rpp   30.  40. -100.  -50.   30.  40.
211 rpp   30.  40.   50.  100.  -40. -30.
212 rpp   30.  40. -100.  -50.  -40. -30.
213 rpp  -40. -30.   50.  100.   30.  40.
214 rpp  -40. -30. -100.  -50.   30.  40.
215 rpp  -40. -30.   50.  100.  -40. -30.
216 rpp  -40. -30. -100.  -50.  -40. -30.
c   -----------------------------------
300 rpp  -60.  60. -100.  100.  -60.  60.
400 rpp  -40.  40. -80.   80.   -40.  40.

nps  5e7
imp:n  1 1m 8 80 0
sdef wgt=8000. x=d1 y=d2 z=d3
si1  -10. 10.
sp1  0  1
si2  -10. 10.
sp2  0  1
si3  -10. 10.
sp3  0  1
mgopt f 1 0
m1 99002.00m 1.
print
f205:n   5. 95. 35. 5
f215:n  15. 95. 35. 5
f225:n  25. 95. 35. 5
f235:n  35. 95. 35. 5
f245:n  45. 95. 35. 5
f255:n  55. 95. 35. 5
```

Libraries

‘xs1’

```
99001.00m 9.99999E+09 0.00000E+00   20030102
xsecs for OECD benchmarks - geometries with voids



       11    99001        0        0        1        0        0        0
        0        1        0        1        0        0        0        0
        1        3        4        5        6        7        0        0
        0        0        0        0        8        0        0       10
       11        0        0        0        0        0        0        0
        0        0        0        0        0        0        0        0
                  50                  100                  1                   0
                   0                    1                  1                   9
                   0                    0                  0
```

‘xs2’

```
99002.00m 9.99999E+09 0.00000E+00   20030102
xsecs for OECD benchmarks - geometries with voids



       11    99002        0        0        1        0        0        0
        0        1        0        1        0        0        0        0
        1        3        4        5        6        7        0        0
        0        0        0        0        8        0        0       10
       11        0        0        0        0        0        0        0
        0        0        0        0        0        0        0        0
                  50                  100                  1                   0
                   0                    1  5.000000000000E-01                   9
  5.000000000000E-01                    0                  0
```

‘dir’

```
atomic weight ratios
 99001 9.99999E+09   99002 9.99999E+09
directory
 99001.00m  9.99999E+09 xs1      0 1 1   11
 99002.00m  9.99999E+09 xs2      0 1 1   11
```